

Dimension-six anomalous $tq\gamma$ couplings in $\gamma\gamma$ collision at the LHC

S. C. İnan*

Department of Physics, Cumhuriyet University, 58140, Sivas, Turkey

Abstract

We have investigated the flavor changing top quark physics on the dimension-six anomalous $tq\gamma$ ($q = u, c$) couplings through the process $pp \rightarrow p\gamma\gamma p \rightarrow pt\bar{q}p$ at the LHC by considering different forward detector acceptances. In this paper, we have taken into account and examine the effects of top quark decay. The sensitivity bounds on the anomalous couplings and, $t \rightarrow q\gamma$ branching ratio have been obtained at the 95% confidence level for the effective lagrangian approach. Besides, we have investigated the effect of the anomalous couplings on single top quark spin asymmetry.

arXiv:1410.3609v1 [hep-ph] 14 Oct 2014

*sceminan@cumhuriyet.edu.tr

I. INTRODUCTION

Top quark mass is at the electroweak symmetry-breaking scale. It is the heaviest elementary particle in the Standard Model (SM), one of the least known [1–3]. Therefore, the top quark properties and its interactions provide a possibility for examining new physics beyond the SM. Moreover, the affects of new physics theories on the top quark interactions are considered to be larger than any other particles [4]. Such anomalous couplings would alter top production and decay at colliders. The most widely studied cases are top quark anomalous interactions via Flavour-Changing Neutral Currents (FCNC). Tree level FCNC decays $t \rightarrow q\gamma$ ($q = u, c$) is not possible in the SM. These decays can only make loop contributions and highly suppressed due to Glashow-Iliopoulos-Maiani (GIM) mechanism. Therefore, $t \rightarrow q\gamma$ branching ratio is very small ($\approx 10^{-14}$) [5–8]. In this instance conflicts with the SM expectations of these decays would be evidence of new physics. Hence, those kind of decays have been studied in various new physics models beyond the SM such as the quark-singlet model [8–10], the two-Higgs doublet model [11–16], the minimal supersymmetric model [17–23], supersymmetry [24], the top-color-assisted technicolor model [25] or extra dimensional models [26, 27].

Present constraints on the FCNC $tq\gamma$ couplings come from the following experimental bounds: The CDF collaboration limits on the branching ratios at 95% C. L. for the process $t \rightarrow q\gamma$ is $BR(t \rightarrow u\gamma) + BR(t \rightarrow c\gamma) < \%3.2$ [28]. The ZEUS collaboration provide at 95% C.L. on the anomalous $tq\gamma$ couplings $\kappa_{tq\gamma} < 0.12$ [29] with the assumption of $m_t = 175$ GeV. The Large Hadron Collider (LHC) can produce number of top quarks in it is of the order of millions per year. Therefore, top quark couplings can be probed with very high sensitivity. In particular, both the ATLAS and CMS collaboration have presented their sensitivity bounds on these rare top quark decays induced by the anomalous FCNC interactions [30–32]. The most stringent experimental bounds recently have been obtained at 95% C.L. by the CMS Collaboration as $BR(t \rightarrow u\gamma) = \%0.0161$ and $BR(t \rightarrow c\gamma) = \%0.182$ [33]. The CMS group have distinguished the $tu\gamma$ and $tc\gamma$ couplings with applying charge ratio method [34] in their process. Since the fact that the u-quark parton distribution function is bigger than the c-quark, they have obtained less sensitivity to $tc\gamma$ coupling.

The new physics effects to FCNC top quark couplings can be obtained in a model independent way by means of the effective operator formalism. The theoretical basis of that

kind of a method really on the assumption that the SM of particle physics is the low-energy limit of a more fundamental theory. Such a procedure is quite general and independent of the new interactions at the new physics energy scale. In order to Buchmller and Wyler [35], these effective operators obey the $SU(2)_L \times U(1)_Y$ gauge symmetries of the SM and, can be written in following form,

$$L = L_{SM} + \frac{1}{\Lambda} L^{(5)} + \frac{1}{\Lambda^2} L^{(6)} + O\left(\frac{1}{\Lambda^3}\right) \quad (1)$$

where, Λ is the energy scale of new physics, L_{SM} is the SM Lagrangian, $L^{(5)}$ and $L^{(6)}$ are all of the dimension five and six operators. As mentioned before, they are invariant under the gauge symmetries of the SM. The five dimensional terms break conservation of lepton and baryon number. Hence, we do not take into account these operators in this paper. The list of $L^{(6)}$ terms is quite vast. In Refs. [36–40], the authors have investigated all dimension six flavor changing effective operators of the FCNC top physics. They have indicated that the criteria in choosing these operators were that they contributed only to tqg (g:gluon) and tqV ($V : \gamma, Z$) FCNC interactions. In this paper, we examine the dimension six operators that give rise to flavor changing interactions of the top quark in the electromagnetic interactions. These operators can be written as shown in [39, 40],

$$\begin{aligned} O_{tB} &= i \frac{\alpha_{it}^B}{\Lambda^2} (\bar{u}_R^i \gamma^\mu D^\nu t_R) B_{\mu\nu}, \\ O_{tB\phi} &= \frac{\beta_{it}^B}{\Lambda^2} (\bar{q}_L^i \sigma^{\mu\nu} t_R) \tilde{\phi} B_{\mu\nu}, \\ O_{tW\phi} &= \frac{\beta_{it}^W}{\Lambda^2} (\bar{q}_L^i \tau^I \sigma^{\mu\nu} t_R) \tilde{\phi} W_{\mu\nu}^I, \end{aligned} \quad (2)$$

where α_{it}^B , β_{it}^B and β_{it}^W dimensionless complex coupling constants, u_R and q_L show the right-handed u-quark singlet and left-handed doublet. $B_{\mu\nu}$ and $W_{\mu\nu}^I$ are the $U(1)_Y$ and $SU(2)_L$ field tensors, respectively. ϕ is the SM Higgs doublet, τ^I are the Pauli matrices and $\tilde{\phi}$ charge conjugate of the Higgs doublet ($\tilde{\phi} = i\tau^2 \phi^*$). Obviously, these operators contribute to t quark anomalous FCNC interactions including photon and Z boson when the partial derivative of D_μ , the Higgs field ϕ and its vacuum expectation value ν are used in the Eqs. (2), through the well-known Weinberg rotation. Moreover, the Z boson couple with the Higgs field. Therefore, there are several extra effective operators which will only contribute to

new FCNC interactions of the Z boson. [36, 37]. These operators will not be considered in this paper as we analyse only $tq\gamma$ anomalous interactions. The FCNC photon and Z boson couplings with t -quark can be isolated defining new coupling constants,

$$\begin{aligned}
\alpha^\gamma &= \cos\theta_W\alpha^B \\
\alpha^Z &= -\sin\theta_W\alpha^B \\
\beta^\gamma &= \sin\theta_W\beta^W + \cos\theta_W\beta^B \\
\beta^Z &= \cos\theta_W\beta^W - \sin\theta_W\beta^B.
\end{aligned} \tag{3}$$

After these definition, the Feynman rules including quartic vertex can be obtained as follows [39, 40]

$$\begin{aligned}
\Gamma_{\gamma t\bar{q}} &= \frac{1}{\Lambda^2}[\gamma_\mu\gamma_R(\alpha_{tj}p_2 + \alpha_{jt}^*p_1) + \hat{v}\sigma_{\mu\nu}(\beta_{tj}\gamma_R + \beta_{jt}^*\gamma_L)](k^\mu g^{\nu\alpha} - k^\nu g^{\mu\alpha}) \\
\Gamma_{\gamma\bar{t}q} &= \frac{1}{\Lambda^2}[\gamma_\mu\gamma_R(\alpha_{tj}p_1 + \alpha_{jt}^*p_2) + \hat{v}\sigma_{\mu\nu}(\beta_{tj}\gamma_R + \beta_{jt}^*\gamma_L)](k^\mu g^{\nu\alpha} - k^\nu g^{\mu\alpha}) \\
\Gamma_{\gamma\gamma t\bar{q}} &= \frac{g_e}{\Lambda^2}[(k_1g_{\mu\nu} - k_{1\nu}\gamma_\mu)\gamma_R(\alpha_{jt} + \alpha_{tj}^*) + (k_2g_{\mu\nu} - k_{1\mu}\gamma_\nu)\gamma_R(\alpha_{jt} + \alpha_{tj}^*)]
\end{aligned} \tag{4}$$

Here, $\sigma_{\mu\nu} = \frac{1}{2}[\gamma_\mu, \gamma_\nu]$, $\gamma_{L(R)}$ are the left(right)-handed projection operators, $\hat{v} = v/\sqrt{2} = 174$ GeV, $g_e = \sqrt{4\pi\alpha}$, k is the photon momentum, p_1 , p_2 are t and $q = u, c$ quark momentums, respectively. In $\Gamma_{\gamma t\bar{q}}$ and $\Gamma_{\gamma\gamma t\bar{q}}$ t -quark (q -quark) is incoming (outgoing) the vertex, in $\Gamma_{\gamma\bar{t}q}$ t -quark (q -quark) is outgoing (incoming) the vertex. Additionally, all the photons momentum are incoming to the vertex.

II. PHOTON-PHOTON INTERACTIONS AT THE LHC

The Large Hadron Collider (LHC) provides high energetic proton-proton collisions with high luminosity. Therefore, it generates very rich statistics data. It is expected that LHC will answer many unknown problems in new theories. However, ultraperipheral interactions and elastic collisions may not be caught at the main detectors at the LHC with limited pseudorapidity. For this reason, ATLAS and CMS Collaborations developed a plan of forward physics with updated extra detectors. These extra detectors are placed at distance of 220 m - 420 m from the interaction point. They provide to detect intact protons which

are scattered after the collisions with some momentum fraction loss $\xi = (|E| - |E'|)/|E|$. Here E is energy of incoming proton and E' is the energy of intact scattered proton. These new machines are known very forward detectors. With these new machines it will be possible to study of exclusive interactions of proton-proton and opens a new opportunities of studying high energy photon-induced reactions such as photon-photon and photon-proton interactions. The pp deep inelastic scattering (DIS) have very complex backgrounds due to interacted protons dissociate into partons. In the DIS process, made up of jets from the proton remnants some ambiguities are occurred which make it hard to detect the new physics signals beyond the SM. On the other hand, $\gamma\gamma$ or γp collisions have a lower backgrounds than proton-proton DIS. Because, in photon induced reactions a quasi-real photons emitted from one proton beams can interact with the other proton or emitted photon. The emitted almost-real photons have a low virtuality. Therefore, the proton structure remains intact. Moreover, $\gamma\gamma$ collisions most clean processes since they do not include any QCD interactions.

Forward detectors can detect intact outgoing protons in the interval $\xi_{min} < \xi < \xi_{max}$. This interval is known as the acceptance of the forward detectors. If the forward detectors are established closer to central detectors, a higher ξ can be obtained. One of the programs about forward detectors was prepared by ATLAS Forward Physics Collaboration (AFP). This program include an acceptance of $0.0015 < \xi < 0.15$, $0.015 < \xi < 0.15$ [41] for the forward detectors. It is organized to two types of measurements to research with high precision using the AFP [42–44]. These are exploratory physics (anomalous couplings between γ and Z or W bosons, exclusive production, etc.) and standard QCD physics (double Pomeron exchange, exclusive production in the jet channel, single diffraction, $\gamma\gamma$ physics, etc.). These measurements will enhance the HERA and Tevatron experiments to the kinematical region of the LHC. Furthermore, CMS-TOTEM forward detectors are placed closer to the central detectors and it has acceptance regions $0.0015 < \xi < 0.5$, $0.1 < \xi < 0.5$ [48, 49]. Main goals of the the TOTEM experiment are examines to the elastic proton-proton interactions, total proton-proton cross-section, and overall types of diffractive physical phenomena. Detectors housed in Roman Pots. It can be moved nearby to the outgoing protons enable to trigger on elastic and diffractive protons and to measure their physical parameters such as the momentum shift and the transverse momentum exchange. Furthermore, detectors of the charged particle in the forward area can catch almost all inelastic physical processes. A large solid angle is covered with support of the CMS detector. Therefore, it is make possible

to precise studies. Moreover, application of forward detectors in conjunction with main detectors with a precise timing, can efficiently decrease backgrounds from pile-up events [50–52].

Photon-photon interactions were recently examined in the measurements of the CDF collaboration [53–59]. Their results are consistent in theoretical calculations with $p\bar{p} \rightarrow p\ell^+\ell^-\bar{p}$ through the subprocess $(\gamma\gamma \rightarrow \ell^+\ell^-)$. Furthermore, the CMS collaboration have detected photon-induced reactions $pp \rightarrow p\gamma\gamma p \rightarrow p\mu^+\mu^-p$, $pp \rightarrow p\gamma\gamma p \rightarrow pe^+e^-p$ from the $\sqrt{s} = 7$ TeV [60, 61]. Therefore, the photon-induced interactions’ potential at the LHC is significant, with its high energetic pp collisions, and high luminosity [62–90].

As mentioned above, forward detectors make it possible to measure high energy photon-photon interactions. This process occurred by two photons radiated off by incoming protons collide and produce a central system X through the process $pp \rightarrow p\gamma\gamma p \rightarrow pXp$. Schematic diagram can be seen for the this process in Fig.1. The system X will be detected by the central detector under clean experimental conditions and the two protons remain intact due to low virtuality of photons. These intact protons also known as forward protons. They can not caught at the main detectors and go on their path near to the beam line. Due to energy loses of the protons can be determined by the forward detectors, it is possible to know invariant mass of the central system $W^2 = 4E^2\xi_1\xi_2$.

At the LHC, the equivalent photon approximation (EPA) has been satisfyingly applied to define processes involving photon exchange with proton beams.[91, 92]. In this method two quasi-real photons with low virtuality ($Q^2 = -q^2$) emitted by each incoming proton interact with each other to produce X through the subprocess $\gamma\gamma \rightarrow X$. The emitted quasi-real photons by the emitters protons with small angles give a spectrum of virtuality Q^2 and the photon energy $E_\gamma = \xi E$. This situation defined by the EPA,

$$\frac{dN}{dE_\gamma dQ^2} = \frac{\alpha}{\pi} \frac{1}{E_\gamma Q^2} \left[\left(1 - \frac{E_\gamma}{E}\right) \left(1 - \frac{Q_{min}^2}{Q^2}\right) F_E + \frac{E_\gamma^2}{2E^2} F_M \right] \quad (5)$$

where m_p is the mass of the proton. The other terms are as follows,

$$Q_{min}^2 = \frac{m_p^2 E_\gamma^2}{E(E - E_\gamma)}, \quad F_E = \frac{4m_p^2 G_E^2 + Q^2 G_M^2}{4m_p^2 + Q^2} \quad (6)$$

$$G_E^2 = \frac{G_M^2}{\mu_p^2} = \left(1 + \frac{Q^2}{Q_0^2}\right)^{-4}, \quad F_M = G_M^2, \quad Q_0^2 = 0.71 \text{GeV}^2. \quad (7)$$

Here, F_E and F_M are functions of the electric and magnetic form factors respectively, $\mu_p^2 = 7.78$ is the squared magnetic moment of the proton. The difference of this spectrum from the pointlike electron case is accounted for by the electromagnetic form factors. The luminosity spectrum of photon-photon collisions $\frac{dL^{\gamma\gamma}}{dW}$ can be obtained in the framework of the EPA as follows,

$$\frac{dL^{\gamma\gamma}}{dW} = \int_{Q_{1,min}^2}^{Q_{max}^2} dQ_1^2 \int_{Q_{2,min}^2}^{Q_{max}^2} dQ_2^2 \int_{y_{min}}^{y_{max}} dy \frac{W}{2y} f_1\left(\frac{W^2}{4y}, Q_1^2\right) f_2(y, Q_2^2). \quad (8)$$

Here we have taken the $Q_{max}^2 = 2 \text{ GeV}^2$ since Q_{max}^2 greater than 2 GeV^2 does not make a significant contribution to this integral. From Eq.(8) the cross section for the main process $pp \rightarrow p\gamma\gamma p \rightarrow pXP$ can be found by integrating $\gamma\gamma \rightarrow X$ subprocess cross section over the photon spectrum:,

$$d\sigma = \int \frac{dL^{\gamma\gamma}}{dW} d\hat{\sigma}_{\gamma\gamma \rightarrow X}(W) dW. \quad (9)$$

In this paper, we have examined anomalous FCNC interactions for the process $pp \rightarrow p\gamma\gamma p \rightarrow pt\bar{q}p$ at the LHC through the subprocess $\gamma\gamma \rightarrow t\bar{q}$. In all the results presented in this work, we impose a cut of $|\eta| < 2.5$ and $p_t > 30 \text{ GeV}$. The QED two-photon survival probability have been taken as 0.9 [93]. In addition to these, we have assumed that the center-of-mass energy of the LHC is 14 TeV.

III. NUMERICAL ANALYSIS

The effective operator methods provide to obtain the possible rare decays of the top in a model-independent manner. The squared amplitude for top FCNC decays $t \rightarrow \gamma q$ ($q = u, c$) can be obtained in terms of the anomalous couplings defined by Eq.(4)

$$|M_{t \rightarrow \gamma q}|^2 = \frac{m_t^4}{2\Lambda^4} m_t^2 |\alpha_{tu}^\gamma + (\alpha_{ut}^\gamma)^*|^2 + 16\hat{v}^2 (|\beta_{tu}^\gamma|^2 + |\beta_{ut}^\gamma|^2) + 8\hat{v}m_t \text{Im}[\beta_{tu}^\gamma (\alpha_{ut}^\gamma + (\alpha_{ut}^\gamma)^*)]. \quad (10)$$

From this result, it is easy to obtain decay width,

$$\Gamma_{t \rightarrow \gamma q} = \frac{m_t^3}{64\pi\Lambda^4} \{m_t^2 |\alpha_{tu}^\gamma + (\alpha_{ut}^\gamma)^*|^2 + 16\hat{v}^2 (|\beta_{tu}^\gamma|^2 + |\beta_{ut}^\gamma|^2) + 8\hat{v}m_t \text{Im}[\beta_{tu}^\gamma (\alpha_{ut}^\gamma + (\alpha_{ut}^\gamma)^*)]\} \quad (11)$$

There are five Feynman Diagrams for the $\gamma\gamma \rightarrow t\bar{q}$ as shown in Fig. 2. The polarization summed amplitude square can be obtained by using Eq.(4),

$$\begin{aligned}
|M_{\gamma\gamma \rightarrow t\bar{q}}|^2 &= \frac{g_e^2 Q_t^2 s}{\Lambda^4 t - m_t^2} t(u - m_t^2) u \{m_t^{10}(t + u) - 12m_t^8 tu + m_t^6(t + u)(t^2 + 13tu + u^2) \\
&\quad - m_t^4 tu(t^2 + 24tu + 7u^2) + 12m_t^2 t^2 u^2(t + u) - 6t^3 u^3\} \{m_t^2 |\alpha_{tu}^\gamma + (\alpha_{ut}^\gamma)^*|^2 \\
&\quad + 16\hat{v}^2 (|\beta_{tu}^\gamma|^2 + |\beta_{ut}^\gamma|^2) + 8\hat{v}m_t \text{Im}[\beta_{tu}^\gamma (\alpha_{ut}^\gamma + (\alpha_{ut}^\gamma)^*)]\}. \tag{12}
\end{aligned}$$

The cross section for the $\gamma\gamma \rightarrow t\bar{q}$ can be written by means of the decay rate as seen from the Eqs.(11) and (12),

$$\frac{d\sigma}{d(\cos\theta)} = \frac{3(s - m_t^2) Q_t^2 g_e^2}{2m_t^3 stu(t - m_t^2)(u - m_t^2)} G_{\gamma\gamma} \Gamma_{t \rightarrow q\gamma}, \tag{13}$$

Here $G_{\gamma\gamma}$ function given as follows,

$$\begin{aligned}
G_{\gamma\gamma} &= m_t^{10}(t + u) - 12m_t^8 tu + m_t^6(t + u)(t^2 + 13tu + u^2) \\
&\quad - m_t^4 tu(t^2 + 24tu + 7u^2) + 12m_t^2 t^2 u^2(t + u) - 6t^3 u^3. \tag{14}
\end{aligned}$$

In figures 3(a-c), we show the total cross sections as functions of branching ratio of the $t \rightarrow q\gamma$ decay for three acceptance regions: $0.0015 < \xi < 0.5$, $0.0015 < \xi < 0.15$ and $0.015 < \xi < 0.15$. We obtain from this figure that total cross sections for the $0.0015 < \xi < 0.5$ better than the others. Also, we have calculated the cross section for the $0.1 < \xi < 0.5$ acceptance range. However, the cross section for the this acceptance range is very small. For instance, it have been obtained 2.75×10^{-5} fb for $BR(t \rightarrow q\gamma) = 0.0005$. Hence, we do not show the cross section for this acceptance range. This result can be understood from the figures 4(a-c). These figure represent the cross sections versus the minimum transverse momenta (or p_{tcut}) of the final quarks for $BR(t \rightarrow q\gamma) = 0.0005$. When Figs. 4(a) and 4(b) are compared, it can be obtained that the acceptance region $1 < \xi < 0.5$ has almost the same result as the region $0.0015 < \xi < 0.5$ with $p_{t,min} = 800$ GeV. Therefore, a high lower bound of the acceptance region behaves an extra p_t cut. In figures 5 (a-c) we plot the p_t distribution of the final state quarks for differential cross section with $BR(t \rightarrow q\gamma) = 0.0005$ for three acceptance regions: $0.0015 < \xi < 0.5$, $0.0015 < \xi < 0.15$ and $0.015 < \xi < 0.15$. It turns out that

anomalous coupling is the dominant effect in low p_t regions. Hence, $0.1 < \xi < 0.5$ forward detector acceptance range is not convenient for the searching dimension-six anomalous top quark coupling.

We have found 95% confidence level (C.L.) limits on the branching ratio of the top quark. We have applied the Poisson distribution statistical analysis method since the SM background for this process is absent. In Poisson analysis, the number of observed events are assumed to be equal to the SM prediction. Upper bounds of events number N_{up} can be obtained from the following equations at the 95% C.L. [94, 95],

$$\sum_{k=0}^{N_{obs}} P_{Poisson}(N_{up}, k) = 0.05. \quad (15)$$

Depending on the number of observed events, values for upper limits N_{up} can be found in Table 38.3 in Ref.[96]. Since $N_{obs} = 0$ in our paper, the N_{up} is obtained equivalent to 3. The N_{up} can be directly converted to the bounds of branching ratios of $t \rightarrow q\gamma$ with using Eq.(13). In Figs.6(a-c), we represent sensitivity bounds on the $BR(t \rightarrow q\gamma)$. These bounds are given as a function of integrated LHC luminosity for three forward detector acceptances $0.0015 < \xi < 0.5$, $0.0015 < \xi < 0.15$ and $0.015 < \xi < 0.15$. We see from this figure that our limits are better than current experimental best stringent result for $t \rightarrow c\gamma$. Also, our results comparable with best LHC limits for $t \rightarrow u\gamma$. At the same time, even at the next searches of the LHC pp collisions with 3000 fb^{-1} of integrated luminosity, LHC sensitivity bounds on $BR(t \rightarrow q\gamma)$ would not be improved substantially [97, 98]. Therefore, it may be important to examine FCNC anomalous coupling of the top quark at future photon-induced LHC studies with very high luminosity values.

On the other hand, FCNC Lagrangian considered in [99, 100] to define dimension-six anomalous interaction contains two effective operators instead of four ones,

$$L_{\gamma tq} = -g_e \bar{q} \frac{i\sigma^{\mu\nu} q_\nu}{m_t} (\lambda^L \gamma_L + \lambda^R \gamma_R) t A_\mu + H.c.. \quad (16)$$

This lagrangian includes the same physics, under change of variables plus some redefinitions of fermion operator coefficients. Nevertheless, the Eq.(16) do not include the quartic vertices. With using this effective lagrangian, decay widths for $t \rightarrow q\gamma$ can obtain much simpler form,

$$\Gamma(t \rightarrow q\gamma) = \frac{g_e^2 m t}{16\pi} (|\lambda^R|^2 + |\lambda^L|^2). \quad (17)$$

The differential cross section is also same as Eq.(13). Therefore, our discussion do not change for this effective lagrangian. Additionally, we have obtained %95 C.L. contours for λ^R and λ^L for $L = 50fb^{-1}$, $L = 100fb^{-1}$, $L = 200fb^{-1}$ and three forward detectors acceptance regions $0.0015 < \xi < 0.5$, $0.0015 < \xi < 0.15$ and $0.015 < \xi < 0.15$ in the Figs.7(a-c). It can be considered that, there is a SM background as $pp \rightarrow p\gamma\gamma p \rightarrow pWb\bar{q}p$. However, the SM cross section is very small ($\sim 10^{-5}$ fb) and, therefore it does not need to take into account.

Furthermore, we have the calculated spin asymmetry of the final state single top quark with using Eq.(16). The correlation among the top spin and its decay products can be obtained in the rest frame of the final state top quark. In this situation, the angular distribution of decay is obtained as follows,

$$\frac{1}{\Gamma_T} \frac{d\Gamma}{d\cos\theta_i} = \frac{1}{2}(1 + \alpha_i \cos\theta_i), \quad (18)$$

where, θ_i angle between the decay product and the top quark spin quantization axis and α_i is the correlation degree between the decay products and top spin ($\alpha_i = 1$ for $i = l^+, \bar{d}, \bar{s}$; $\alpha_i = 0.4$ for $i = b$) [101]. If there are a mixture of spin up and spin down top quarks in the interaction, the Eq.(19) turns into following form,

$$\frac{1}{\Gamma_T} \frac{d\Gamma}{d\cos\theta_i} = \frac{1}{2}(1 + A\alpha_i \cos\theta_i). \quad (19)$$

Here, A is called the spin asymmetry. In order to find the cross section, depending on the spin, the following projection operator can be used,

$$\sum_{s_t} u(p_1, s_t)\bar{u}(p_1, s_t) = \frac{1}{2}(1 + \gamma_5 \not{s}_t)(\not{p}_1 + m_t) \quad (20)$$

where s_t is the spin vector of the top quark. It can be obtained in the helicity basis as follows,

$$s_t^\mu = \lambda_t \left(\frac{|\vec{p}_1|}{m_t}, \frac{E_1}{m_t} \frac{\vec{p}_1}{|\vec{p}_1|} \right); \quad \lambda_t = \pm 1, \quad (21)$$

here, E_1 is the energy of the top quark. In this situation, spin asymmetry of the top quark can be written in terms of spin dependent events number $N(\lambda_t)$ as following form,

$$A = \frac{N(\lambda_t = 1) - N(\lambda_t = -1)}{N(\lambda_t = 1) + N(\lambda_t = -1)}. \quad (22)$$

Depending on the helicity of the top quark λ_t , differential cross section can be obtained for $\gamma\gamma \rightarrow t\bar{q}$ subprocess,

$$\begin{aligned} \frac{d\sigma(\lambda_t)}{d(\cos\theta)} &= -\frac{3g_e^4 Q_t^2 (s - mt^2)}{128\pi m t^2 s^2 t u (t - mt^2)^2 (u - mt^2)^2} [(|\lambda^R|^2 + |\lambda^L|^2) 2s G_{\gamma\gamma} \\ &+ \lambda_t (|\lambda^R|^2 - |\lambda^L|^2) H_{\gamma\gamma}], \end{aligned} \quad (23)$$

where,

$$\begin{aligned} H_{\gamma\gamma} &= \frac{1}{t + u} [(16tu)mt^{12} - 4(t + u)(t^2 + u^2 + 12tu)mt^{10} \\ &+ (76tu^3 + 76ut^3 + 176t^2u^2)mt^8 \\ &+ (t + u)(2t^4 + 2u^4 - 47tu^3 - 47ut^3 - 166t^2u^4)mt^6 \\ &+ (9tu^5 + 9ut^5 + 108t^2u^4 + 108u^4t^2 + 222t^3u^3)mt^4 \\ &- (t + u)(19t^2u^4 + 19u^4t^2 + 74t^3u^3)mt^2 + 12t^3u^3(t + u)^2]. \end{aligned} \quad (24)$$

There is no polarization of the top quark when $\frac{|\lambda_R|}{|\lambda_L|} = 1$ as showed from the Eq. 23. In Fig.8, we have plotted the top quark spin asymmetry as functions of the $\frac{|\lambda_R|}{|\lambda_L|}$ for $0.0015 < \xi < 0.5$. We have also obtained the spin asymmetry for $0.0015 < \xi < 0.15$ and $0.015 < \xi < 0.15$. However, since these results very similar to $0.0015 < \xi < 0.5$ case, we do not show the figures for these acceptance ranges. As seen from the Fig.8, when $\frac{|\lambda_R|}{|\lambda_L|}$ goes to 0 (infinity), asymmetry approach the -1 (1). Therefore, asymmetry can be used to determine the type of the interaction lagrangian.

IV. CONCLUSIONS

The LHC can be used as a high energy photon-photon and photon-proton collider with new equipments which is called very forward detectors. There is no existing high energy

photon-photon, photon-proton collider with this quality. Particle production through $\gamma\gamma$ fusion yield fewer backgrounds than the pure DIS process. There are no proton remnants after the collisions and, these type of interactions are electromagnetic in nature. The intact protons detect in forward detectors. These detection provide to measure the energy of the almost-real photons. In this case, it is possible to determine the invariant mass of the central system. With this clean environment, any signal which discrepancy with the prospect of the SM would be a conclusive clue for new physics beyond the SM. Moreover, anomalous $tq\gamma$ couplings might also be uniquely revealed in single top photon-induced reactions [41].

In this paper we have examined anomalous dimension-six top quark photon couplings in a model-independent way in the $pp \rightarrow p\gamma\gamma p \rightarrow pt\bar{q}p$ process for three forward detector acceptances $0.0015 < \xi < 0.5$, $0.0015 < \xi < 0.15$ and, $0.015 < \xi < 0.15$. We have obtained the sensitivity bounds on branching ratio of the $t \rightarrow \gamma q$ and anomalous couplings. We see that, our obtained results can improve the sensitivity bounds with respect to current experimental results. We have also made these analysis for an other dimension-six effective lagrangian which have only two anomalous couplings. This effective operator contain same physics. Therefore, we have obtained same results for the cross sections and sensitivity bounds. Additionally, we have analyzed spin asymmetry of the single top quark through the process $pp \rightarrow p\gamma\gamma p \rightarrow pt\bar{q}p$ for the this effective lagrangian. We have seen that the asymmetry is very sensitive to the couplings. Hence, asymmetry can be used in determining the structure of the interaction lagrangian. As a result, photon-photon fusion provides new opportunities for top quark physics beyond the SM.

-
- [1] M. Beneke et al., hep-ph/0003033;
- [2] D. Chakraborty, J. Konigsberg, and D. Rainwater, *Annu. Rev. Nucl. Part. Sci.* **53**, 301 (2003);
- [3] W. Wagner, *Rep. Prog. Phys.* **68**,2409 (2005).
- [4] J. A. Aguilar-Saavedra, *Nucl. Phys. B* **812**, 181 (2009).
- [5] B. Grzadkowski, J. F. Gunion and P. Krawczyk, *Phys. Lett. B* **268** 106 (1991).
- [6] G. Eilam, J. L. Hewett and A. Soni, *Phys. Rev. D* **44** 1473 (1991).
- [7] G. Couture, C. Hamzaoui and H. Knig, *Phys. Rev. D* **52** 1713 (1995).
- [8] J. A. Aguilar-Saavedra and B. M. Nobre, *Phys. Lett. B* **553** 251(2003).
- [9] F. del Aguila, J. A. Aguilar-Saavedra and R. Miquel, *Phys. Rev. Lett.* **82** 1628 (1999).
- [10] J. A. Aguilar-Saavedra, *Phys. Rev. D* **67** 035003 (2003). Erratum-ibid. *D* **69** 099901 (2004).
- [11] T. P. Cheng and M. Sher, *Phys. Rev. D* **35** 3484 (1987).
- [12] B. Grzadkowski, J. F. Gunion and P. Krawczyk, *Phys. Lett. B* **268** 106 (1991).
- [13] M. E. Luke and M. J. Savage, *Phys. Lett. B* **307** 387 (1993).
- [14] D. Atwood, L. Reina and A. Soni, *Phys. Rev. D* **53** 1199 (1996).
- [15] D. Atwood, L. Reina and A. Soni, *Phys. Rev. D* **55** 3156 (1997).
- [16] S. Bejar, J. Guasch and J. Sola, *Nucl. Phys. B* **600** 21 (2001).
- [17] C. S. Li, R. J. Oakes and J. M. Yang, *Phys. Rev. D* **49** 293 (1994). Erratum-ibid.*D* **56**:3156,(1997).
- [18] G. M. de Divitiis, R. Petronzio and L. Silvestrini, *Nucl. Phys. B* **504** 45 (1997).
- [19] J. L. Lopez, D. V. Nanopoulos and R. Rangarajan, *Phys. Rev. D* **56** 3100 (1997).
- [20] J. Guasch and J. Sola, *Nucl. Phys. B* **562** 3 (1999).
- [21] D. Delepine and S. Khalil, *Phys. Lett. B* **599** 62 (2004).
- [22] J. J. Liu, C. S. Li, L. L. Yang and L. G. Jin, *Phys. Lett. B* **599** 92 (2004).
- [23] J. J. Cao et al., *Phys. Rev. D* **75** 075021 (2007).
- [24] J. M. Yang, B.-L. Young and X. Zhang, *Phys. Rev. D* **58** 055001 (1998).
- [25] G. Lu, F. Yin, X. Wang and L. Wan, *Phys. Rev. D* **68** 015002 (2003).
- [26] G. P. K. Agashe and A. Soni, *Phys. Rev. D* **71** 016002 (2005).
- [27] G. P. K. Agashe and A. Soni, *Phys. Rev. D* **75** 015002 (2007).
- [28] F. Abe et al., (CDF Collaboration), *Phys. Rev. Lett.* **80** 2525-2530 (1998).

- [29] ZEUS Collaboration, Phys. Lett. B, **708** 27-36 (2012).
- [30] J. Carvalho et al., (ATLAS Collaboration), Eur. Phys. J. C **52** 999-1019 (2007).
- [31] L. Benucci, A. Kyriakis, Nucl. Phys. Proc. Suppl. 177-178 (2008) 258-260.
- [32] Efe Yazgan et al., arXiv:1312.5435.
- [33] CMS Collaboration, CMS-PAS-TOP-14-003
- [34] S. Khatibi and M. Mohammadi Najafabadi, Phys. Rev. D **89** 054011 (2014).
- [35] W. Buchmüller and D. Wyler, Nucl. Phys. B268, 621 (1986).
- [36] P. M. Ferreira, O. Oliveira, and R. Santos, Phys. Rev. D **73**, 034011 (2006).
- [37] P. M. Ferreira and R. Santos, Phys. Rev. D **73**, 054025 (2006).
- [38] P. M. Ferreira and R. Santos, Phys. Rev. D **74**, 014006 (2006).
- [39] P. M. Ferreira, R. B. Guedes and R. Santos, Phys. Rev. D **77** 114008 (2008).
- [40] R. A. Coimbra *et al.*, Phys. Rev. D **77** 014006 (2009).
- [41] M. Albrow *et al.*, (FP420 R and D Collaboration), J. Instrum. **4**, T10001 (2009).
- [42] ATLAS Collaboration, Tech. Rep. CERN-LHCC-2011- 012. LHCC-I-020, (2011).
- [43] L. Adamczyk *et al.*, Tech. Rep. ATLCOM- LUM-2011-006, CERN, 2011.
- [44] O. Kepka *et al.*, Tech. Rep. ATL-COM-PHYS-2012-775, CERN, (2011).
- [45] G. Antchev *et al.* (The TOTEM Collaboration), EPL 96 21002, (2011).
- [46] G. Antchev *et al.* (The TOTEM Collaboration), EPL 98 31002, (2012).
- [47] G. Antchev *et al.* (The TOTEM Collaboration), CERNPH-EP-2012-239, (2012).
- [48] O. Kepka and C. Royon, Phys. Rev. D **78**, 073005 (2008).
- [49] V. Avati and K. Osterberg, Report No. CERN-TOTEM-NOTE-2005-002, (2006).
- [50] [22] M. G. Albrow et al. (FP420 R and D Collaboration), JINST 4, T10001 (2009).
- [51] M. Tasevsky, Nucl. Phys. Proc. Suppl. 179-180, 187 (2008).
- [52] M. G. Albrow, T. D. Coughlin and J. R. Forshaw, Prog. Part. Nucl. Phys. **65**, 149 (2010)
- [53] A. Abulencia *et al.*, (CDF Collaboration), Phys. Rev. Lett. **98**, 112001 (2007).
- [54] T. Aaltonen *et al.*, (CDF Collaboration), Phys. Rev. Lett. **99**, 242002 (2007).
- [55] T. Aaltonen *et al.*, (CDF Run II Collaboration), Phys. Rev. D **77**, 052004 (2008).
- [56] T. Aaltonen *et al.*, (CDF Collaboration), Phys. Rev. Lett. **102**, 242001 (2009).
- [57] T. Aaltonen *et al.*, (CDF Collaboration), Phys. Rev. Lett. **102**, 222002 (2009).
- [58] O. Kepka and C. Royon, Phys. Rev. D **76**, 034012 (2007).
- [59] M. Rangel, C. Royon, G. Alves, J. Barreto and R. Peschanski, Nucl. Phys. B **774**, 53 (2007).

- [60] S. Chatrchyan *et al.*, (CMS Collaboration), JHEP **1201**, 052 (2012).
- [61] S. Chatrchyan *et al.*, (CMS Collaboration), JHEP **1211**, 080 (2012).
- [62] V. Khoze, A. Martin, R. Orava and M. Ryskin, Eur. Phys. J. **C19**, 313 (2001).
- [63] M. Albrow, T. Coughlin and J. Forshaw, Prog. Part. Nucl. Phys. **65**, 149 (2010).
- [64] I. F. Ginzburg and A. Schiller, Phys. Rev. D **57**, R6599 (1998).
- [65] I. F. Ginzburg and A. Schiller, Phys. Rev. D **60**, 075016 (1998).
- [66] S. Lietti, A. Natale, C. Roldao and R. Rosenfeld, Phys. Lett. B **497**, 243 (2001).
- [67] K. Piotrkowski, Phys. Rev. D **63**, 071502(R) (2001).
- [68] V. Goncalves and M. Machado, Phys. Rev. D **75**, 031502(R) (2007).
- [69] M. Machado, Phys. Rev. D **78**, 034016 (2008).
- [70] S. Atağ, S. C. İnan and İ. Şahin, Phys. Rev. D **80**, 075009 (2009).
- [71] İ. Şahin and S. C. İnan, JHEP **09**, 069 (2009).
- [72] S. C. İnan, Phys. Rev. D **81**, 115002 (2010).
- [73] E. Chapon, C. Royon and O. Kepka, Phys. Rev. D **81**, 074003 (2010).
- [74] S. Atağ and A. Billur, JHEP **11** 060 (2010).
- [75] İ. Şahin and A. Billur, Phys. Rev. D **83**, 035011 (2011).
- [76] İ. Şahin and M. Köksal, JHEP **11**, 100 (2011).
- [77] S. C. İnan and A. Billur, Phys. Rev. D **84**, 095002 (2011).
- [78] R. S. Gupta, Phys. Rev. D **85**, 014006 (2012).
- [79] İ. Şahin, Phys. Rev. D **85**, 033002 (2012).
- [80] L. N. Epele *et al.*, Eur. Phys. J. Plus **127**, 60 (2012).
- [81] İ. Şahin and B. Şahin, Phys. Rev. D **86**, 115001 (2012).
- [82] A. A. Billur, Europhys. Lett. **101**, 21001 (2013).
- [83] H. Sun and C. X. Yue, Eur. Phys. J. C **74**, 2823 (2014).
- [84] H. Sun, Nucl. Phys. B **886**, 691 (2014) arXiv:1402.1817 [hep-ph].
- [85] A. Senol, A. T. Tasci, I. T. Cakir and O. Cakir, arXiv:1405.6050 [hep-ph].
- [86] M. Köksal and S. C. İnan, Adv. High Energy Phys. **2014**, 315826 (2014) [hep-ph].
- [87] M. Köksal and S. C. İnan, Adv. High Energy Phys. **2014**, 315826 (2014)
- [88] H. Sun, arXiv:1407.5356 [hep-ph].
- [89] H. Sun, Y. J. Zhou and H. S. Hou, arXiv:1408.1218 [hep-ph]
- [90] M. Tasevsky, arXiv:1407.8332 [hep-ph]

- [91] V. Budnev, I. Ginzburg, G. Meledin and V. Serbo, Phys. Rep. **15**, 181 (1975).
- [92] G. Baur *et al.*, Phys. Rep. **364**, 359 (2002).
- [93] V. A. Khoze, A. D. Martin and M. G. Ryskin, Eur. Phys. J. C **23**, 311 (2002).
- [94] J. de Favereau de Jeneret, *et al.*, arXiv:0908.2020 [hep-ph].
- [95] T. Pierzchala and K. Piotrkowski, Nucl. Phys. Proc. Suppl. 179-180, 257 (2008)
arXiv:0807.1121 [hep-ph].
- [96] K.A. Olive et al. (Particle Data Group), Chin. Phys. C, **38**, 090001 (2014).
- [97] CMS Collaboration, CMS-PAS-FTR-13-016.
- [98] ATLAS Collaboration, ATL-PAHYS-PUB-2012-001.
- [99] J. A. Aguilar-Saavedra, Nucl. Phys. B, **812**, (2009).
- [100] J. A. Aguilar-Saavedra, Nucl. Phys. B, **837**, (2010).
- [101] G. Mahlon, arXiv:hep-ph/0011349 (2000)

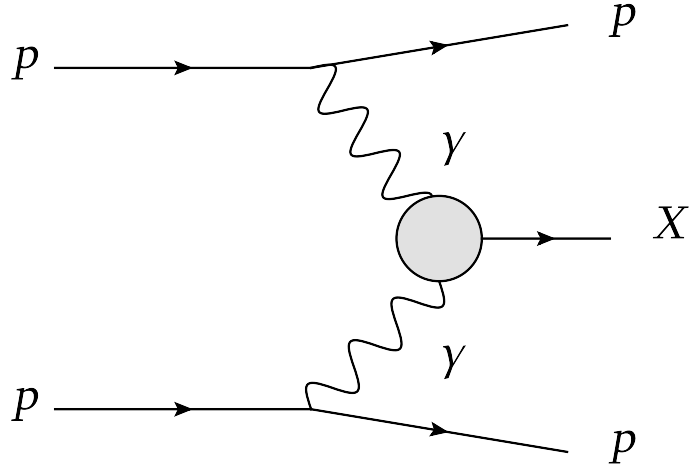


FIG. 1: Schematic diagram for the reaction $pp \rightarrow p\gamma\gamma p \rightarrow pXp$.

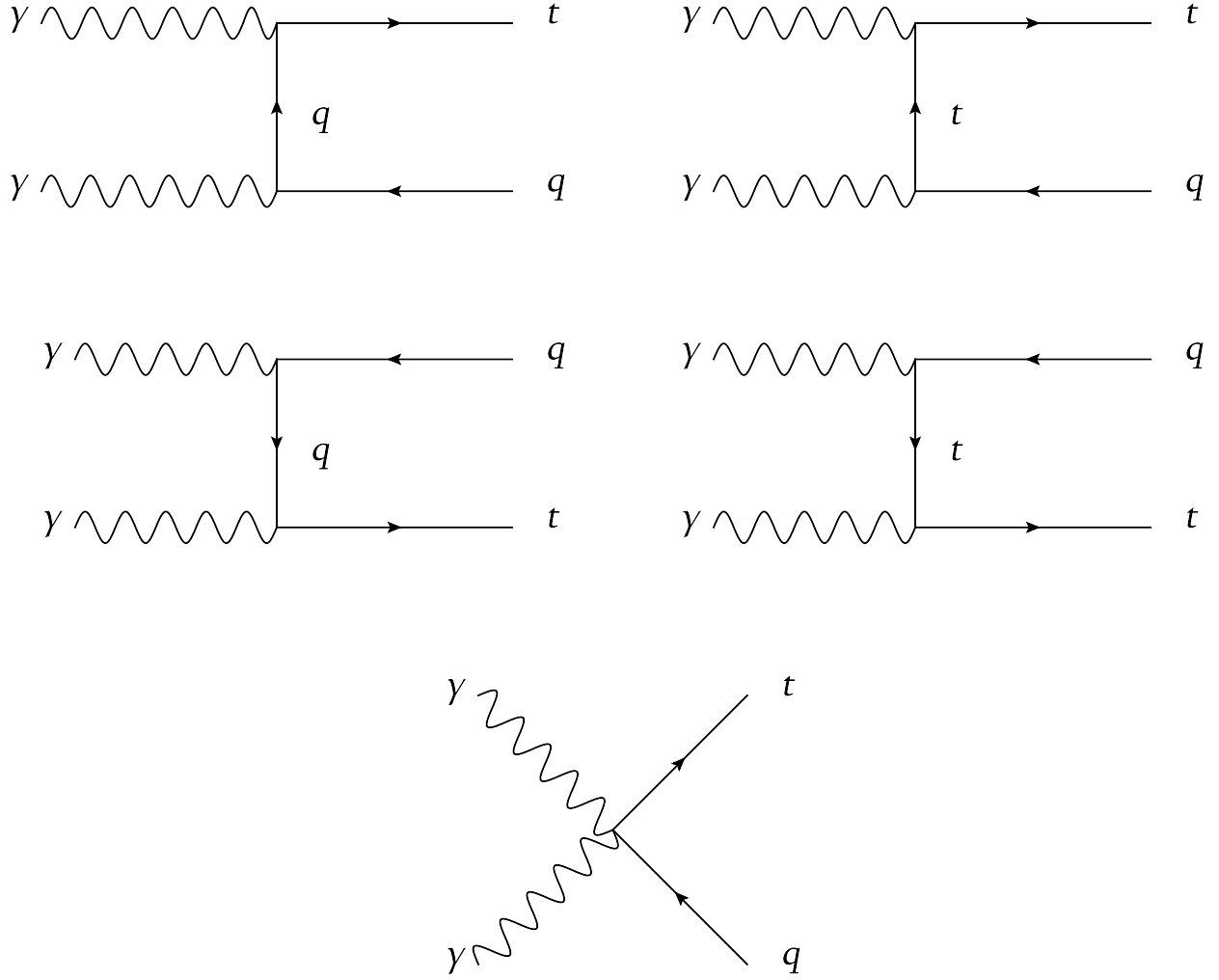


FIG. 2: Three level Feynman diagrams for the subprocess $\gamma\gamma \rightarrow t\bar{q}$ ($q = u, c$) in the presence of the anomalous dimension-six $tq\gamma$ couplings.

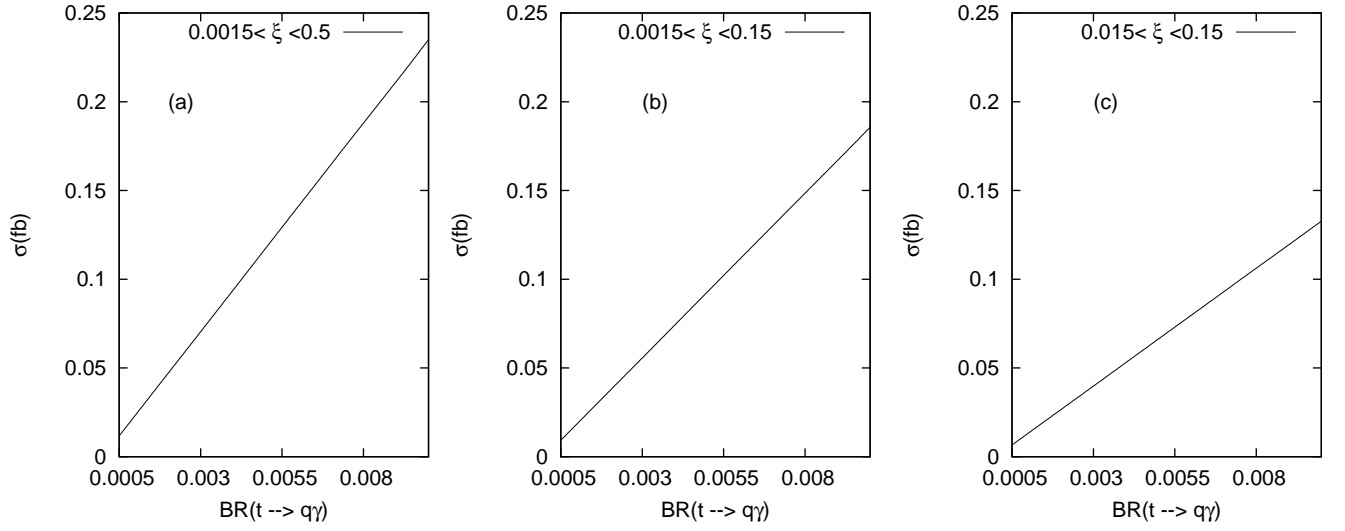


FIG. 3: The cross sections of $pp \rightarrow p\gamma\gamma \rightarrow pt\bar{q}p$ as a function of branching ratios of $t \rightarrow q\gamma$ ($BR(t \rightarrow q\gamma)$) for three forward detector acceptances: $0.0015 < \xi < 0.5$, $0.0015 < \xi < 0.15$ and $0.015 < \xi < 0.15$.

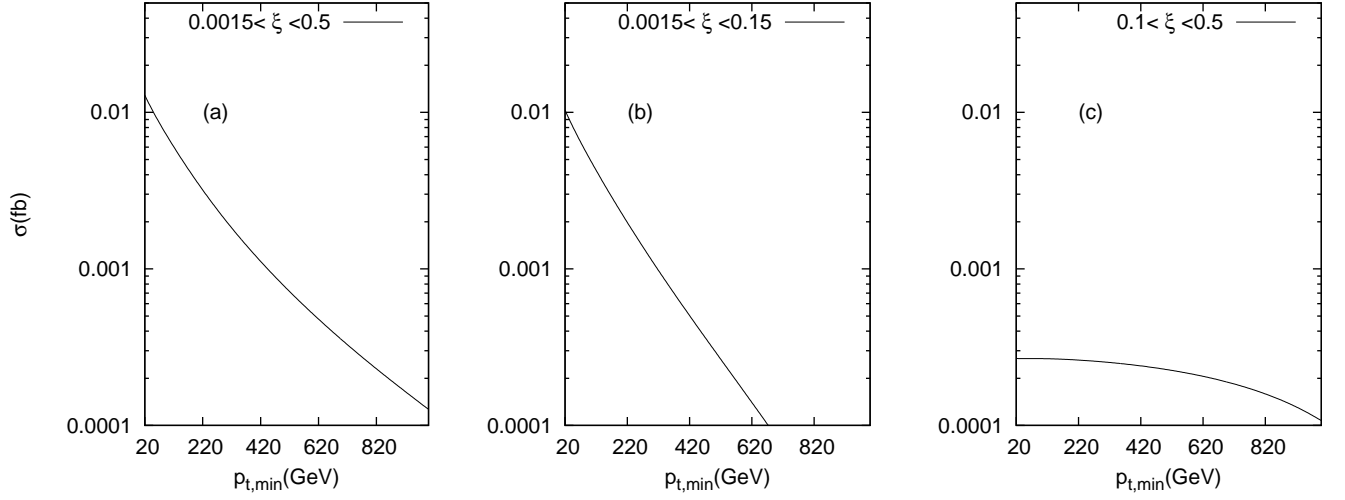


FIG. 4: Cross sections of $pp \rightarrow p\gamma\gamma \rightarrow pt\bar{q}p$ as a function of the transverse momentum cut on the final state particles for $BR(t \rightarrow \gamma q) = 0.0005$ and three forward detector acceptances: $0.0015 < \xi < 0.5$, $0.0015 < \xi < 0.15$, and $0.1 < \xi < 0.5$.

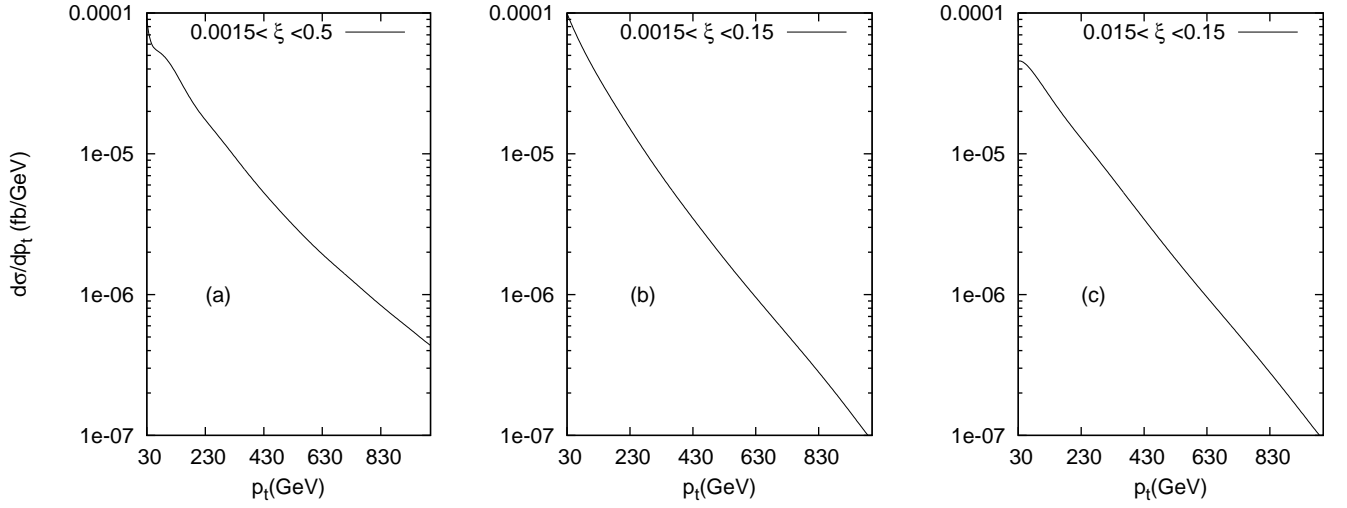


FIG. 5: Differential cross sections of $pp \rightarrow p\gamma\gamma \rightarrow pt\bar{q}p$ as a function of the transverse momentum on the final state particles for $BR(t \rightarrow \gamma q) = 0.0005$ and three forward detector acceptances: $0.0015 < \xi < 0.5$, $0.0015 < \xi < 0.15$, and $0.015 < \xi < 0.15$.

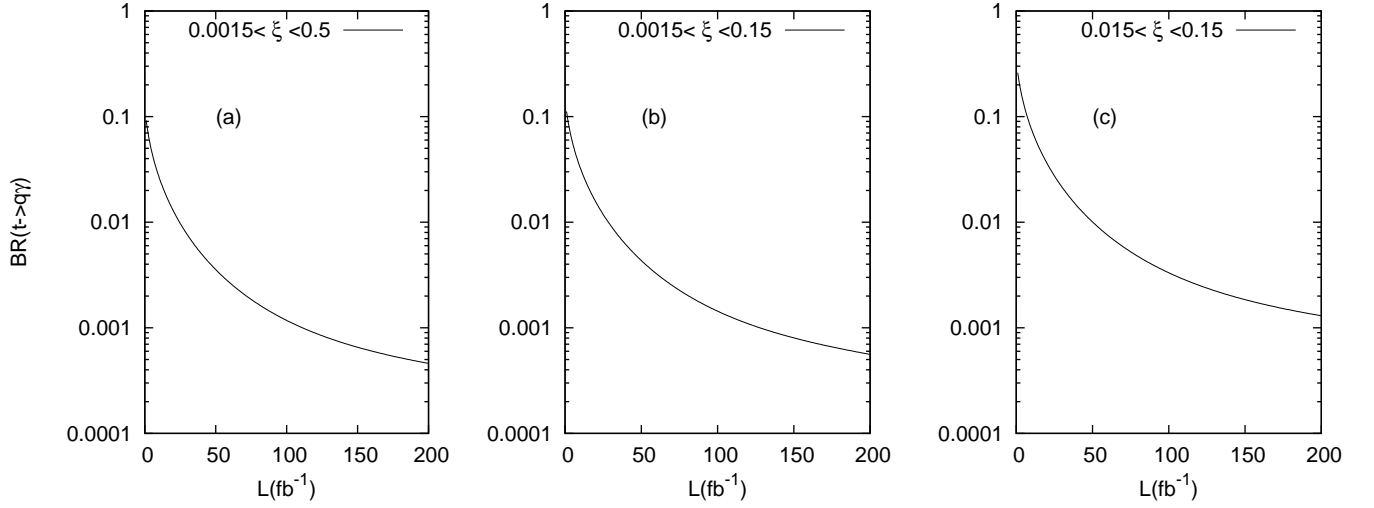


FIG. 6: 95% C.L. lower bounds for branching ratios of $t \rightarrow q\gamma$ ($BR(t \rightarrow q\gamma)$) as a function of integrated LHC luminosity for three forward detector acceptances: $0.0015 < \xi < 0.5$, $0.0015 < \xi < 0.15$ and $0.015 < \xi < 0.15$.

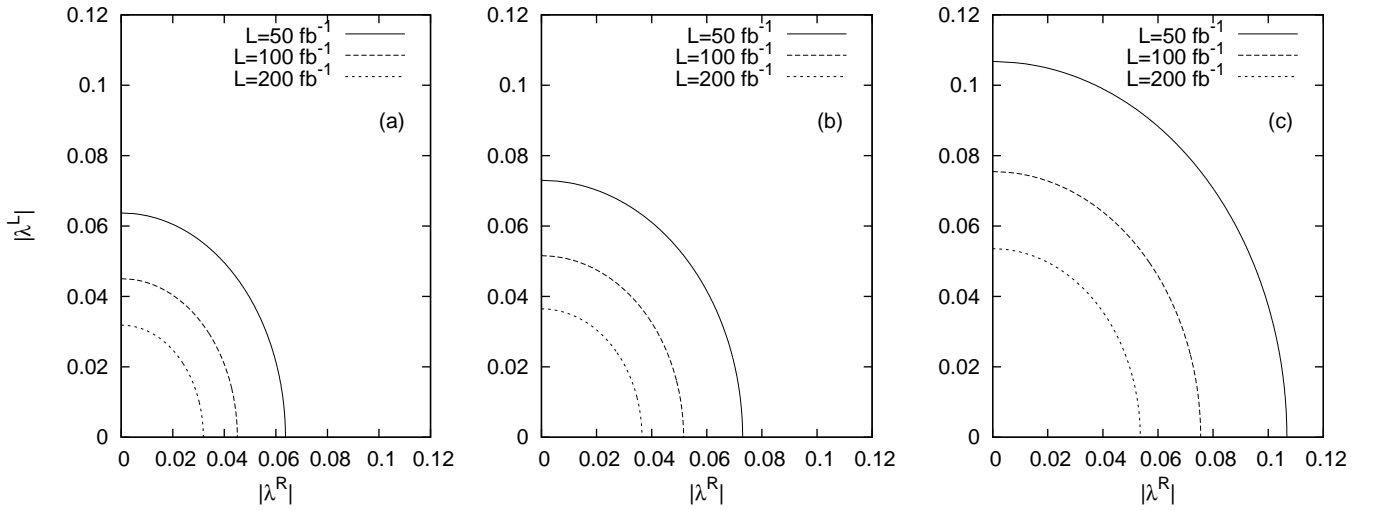


FIG. 7: %95 C.L. contours for $|\lambda^R| - |\lambda^L|$ for $L = 50fb^{-1}$, $L = 100fb^{-1}$, $L = 200fb^{-1}$ and three forward detectors acceptance regions: $0.0015 < \xi < 0.5$, $0.0015 < \xi < 0.15$ and $0.015 < \xi < 0.15$.

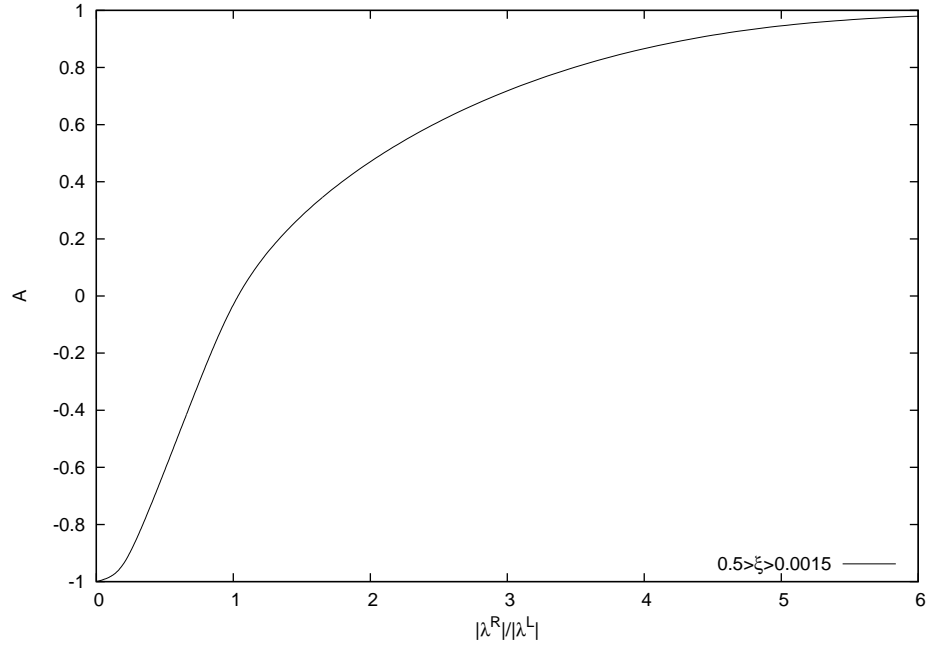


FIG. 8: Single top quark spin asymmetry as function of the $|\lambda^R|/|\lambda^L|$ for $0.0015 < \xi < 0.5$.